

Article

Chemometric Optimisation of a Copper Sulphide Tailings Flocculation Process in the Presence of Clays

Claudia Castillo ^{1,2,*} , Christian F. Ihle ^{1,2}  and Ricardo I. Jeldres ³ 

¹ Laboratory for Rheology and Fluid Dynamics, Department of Mining Engineering, Universidad de Chile, Beauchef 850, Santiago 8370448, Chile; cihle@ing.uchile.cl

² Advanced Mining Technology Center, Universidad de Chile, Tupper 2007, Santiago 8370451, Chile

³ Departamento de Ingeniería Química y Procesos de Minerales, Facultad de Ingeniería, Universidad de Antofagasta, Av. Angamos 601, Antofagasta 1240000, Chile; ricardo.jeldres@uantof.cl

* Correspondence: ccastillo@ing.uchile.cl; Tel.: +562-2978-4991

Received: 21 August 2019; Accepted: 18 September 2019; Published: 26 September 2019



Abstract: The presence of fine and ultra-fine gangue minerals in flotation plants can contribute to sub-optimal valuable ore recovery and incomplete water recycling from thickeners, with the performance of the latter equipment relying on adequate flocculation. In order to study the dependence of the flocculation process on the suspension-flocculant mixing conditions, a series of experiments—chosen using chemometric analysis—were carried out by varying mixing conditions, solid concentration, water salinity and flocculant dosage. To this purpose, two different tailings (both featuring coarse and fine content) were considered and a response surface methodology based on a Doehlert experimental design was used. The results suggest that the operational conditions to optimise the flocculated tailings settling rate and the suspended solids that report to a thickener overflow are not necessarily the same. This is a reasonable outcome, given that the settling rate depends on the coarse aggregates generated in the slurry, while the overflow solids content is governed both by either fine particle content (and its characteristics) or small aggregates. It is inferred that to maximise dewatering performance two stages should be involved—a separate treatment of the thickener overflow to remove fine content and thickening at optimal flocculant dosage to enhance this process.

Keywords: tailings; flocculation; clays; chemometrics analysis

1. Introduction

Water is a scarce commodity for many mining companies, in particular in countries such as Chile, Australia and South Africa, where it is essential to minimise water consumption for massive large-scale operations placed in arid regions [1–3]. The challenge of reducing makeup water volumes in concentrator plants is bonded to the requirement of producing and handling high solid concentrations for their tailings storage facilities [4].

At the heart of most of the copper tailings thickening processes is particle flocculation. Aqueous solutions of flocculants (long chains of water-soluble polymers) are added to bridge the fine particles into large, fast-settling aggregates, with the aim of producing a clear liquor (overflow) and also a concentrated slurry (underflow); the latter is typically pumped out from the cone base of the thickener and then transported to a final tailings storage in deposition areas.

The thickening performance depends on three factors: (i) particle surface chemistry, especially of the fine particle contents, including the most common clays kaolinite and smectite, (ii) water chemistry, including dissolved salts along with both high and low molecular weight additives and (iii) hydrodynamic conditions to promote effective mixing. The interaction of these three factors is

highly complex and a better understanding of them would be extremely useful for large-scale unit design and water management optimisation. The present work aims at contributing in this direction by analysing the aggregate behaviour after flocculation (aggregate size, settling rate and supernatant turbidity) of real copper sulphide tailings, both with and without addition of a clay phase and under different hydrodynamic solid-flocculant mixing conditions. Also, the electrolyte effect on flocculation is analysed.

An example of one of the interactions which has been studied thoroughly in literature is the flocculation of clays, where one of the most common case of study is kaolinite. In this case, fine particles can aggregate in specific ways due to their characteristic surface charge distributions (edges and faces with different charges depending on the pH). Their structure after aggregate formation can be either face-edge (also known as “card-house”), edge-edge or face-face (“card-pack”) depending on the electrolyte characteristics [5–7].

The type of salt (including its ionic strength), in combination with flocculants, is an aspect that defines the characteristics of the particle aggregate and thus the aggregate settling behaviour. The impact of the combination between salt water and flocculant type in flocculation properties has also been reported and, in particular, the significant influence of charge and molecular weight of the polymer in real tailings of predominantly quartz and albite [8], synthetic suspensions of alumina [9] and kaolinite [10].

Regarding the hydrodynamic mixing conditions, both the shear rate and the residence time have an influential role in aggregate stability and size distribution [11,12]. Although this has been extensively studied with focus placed on the thickening process in a theoretical context, there have been fewer efforts to understand the combined problem of maximising both settling rate and overflow clarity within gravity thickeners. Possibly this is because the issue of increasing levels of fine minerals in overflow is relatively recent and is associated in general with finer grinding rates due to the progressively decreasing ore grades.

A comprehensive analysis of the quantitative implications of these input variables on water recirculation capacity and quality would require consideration of realistic mineral blends and flocculant dosing conditions. Even though previous laboratory works on controlled clays flocculation experiments exist (e.g., References [13,14]), the extremely high flocculant dosing and the use of pure minerals preclude a direct extrapolation to real operations. Analogous efforts have been made to characterise the contribution of fine oil sands tailings and clay blends [15].

In the Chilean mining context, there is a specific need to address the combined effect of salts and typical minerals present in local copper tailings on the flocculation stage. Such minerals include quartz and andesite as coarse fractions and kaolinite, illite, muscovite and/or chlorite (e.g., References [16,17]) as finer ones. The liquid phase of those tailings is mixed with flocculants and flotation reagents, whereas it is increasingly common that, instead of freshwater, seawater or brackish water are used [2].

The challenge of testing a representative number of concentrations of a single type of clay (n_1), salt types (n_2), salt concentrations (n_3), mixing rates (n_4) and flocculant dosage (n_5) would require, following a full factorial design, $n_1 \times n_2 \times n_3 \times n_4 \times n_5$ experiments to reproduce all possible combinations. To avoid this potentially prohibitive amount of experimental measurements (especially for prospective testing purposes in metallurgical laboratories at mineral processing plants), the present paper proposes the use of chemometric analysis, defined as “the chemical discipline that uses mathematical, statistical and other methods employing formal logic (a) to design or select optimal measurement procedures and experiments and (b) to provide maximum relevant chemical information by analysing chemical data” [18] to optimise both the distribution and number of tests.

The intent of the present paper is to use the technique described above to analyse the impact of solid content, flocculant dosage, mixing rate and kaolinite content, both on settling rate and the resulting turbidity of the overflow after flocculation.

2. Materials and Methods

2.1. Materials

A copper sulphide tailings (SG 2.74) and kaolin clay (SG 2.47) were used in this study. The copper sulphide tailings sample was collected from a Chilean tailings deposit and dried for three days at 70 °C. The kaolin sample (mined material) was supplied from a local store.

The mineralogy of the kaolin sample, determined using X-ray diffraction (XRD), was 93.5% of kaolinite and 6.5% quartz. The mineral composition of the copper sulphide tailings is shown in Table 1.

Table 1. Mineral composition of the copper sulphide tailings analysed by X-ray diffraction (XRD) (wt.%).

Albite	Chamosite	Quartz	Muscovite	Hematite	Vermiculite
39.1	25.5	20.1	9.4	5.0	1.1

The particle size distribution (PSD) of the tailings and kaolin samples, measured by laser diffraction using a Malvern Mastersizer 2000 instrument, is shown in Figure 1. The copper sulphide tailings had a d_{80} of 84 μm and 26% of the total volume was smaller than 10 μm . The kaolin sample had a d_{80} of 27 μm and 43% of its total volume was smaller than 10 μm .

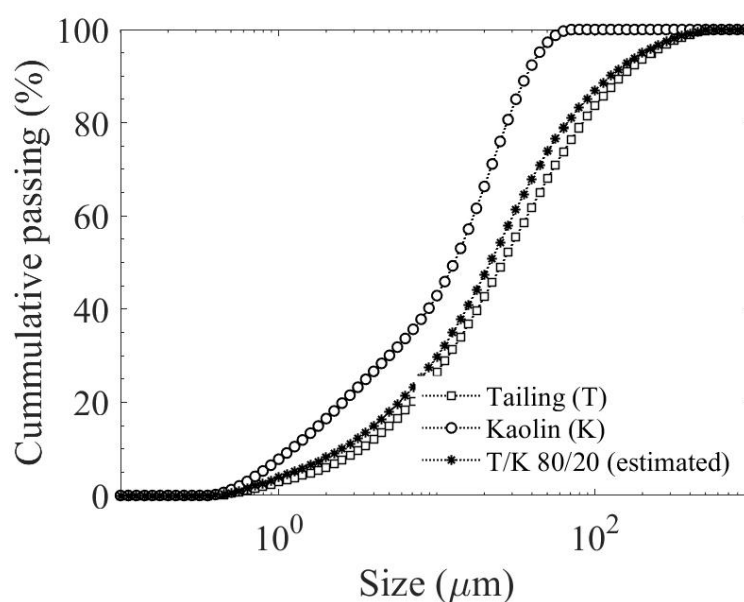


Figure 1. Cumulative distribution of copper sulphide tailings (T), kaolin sample (K) and tailings/kaolin 80/20 mixture (TK).

The flocculant used was a commercial anionic polyacrylamide, SNF[®] 704 supplied by courtesy of SNF Chile S.A., with a molecular weight higher than 18×10^6 g/mol. A 2.5 g/dm³ polymer solution (0.25 wt.%), gently mixed for 24 h, was prepared and used before two weeks after preparation to minimise ageing effects. Within this period, a flocculant aliquot of the polymer solution was diluted in distilled water once a day at 0.25 g/dm³ (0.025 wt.%) for use in the daily test runs.

The solutions—for slurry preparation—used in this study were distilled water, seawater or salts dissolved in distilled water. The salts were NaCl, CaCl₂ and MgCl₂, all of them being analytical reagent grade.

2.1.1. Flocculation Experiments

Flocculation experiments were carried out by dosing flocculant into suspensions (0.45 dm^3) in a 1 dm^3 , 100 mm diameter vessel fitted with four 10 mm-width baffles, symmetrically placed around the vessel periphery. A 50 mm propeller-type (marine) stirrer [19] was placed in downward position, 20 mm above the vessel bottom.

Measurements of chord length distributions (CLD) were made as an approximation of the aggregate size distribution. For this purpose, a Focused Beam Reflectance Measurement (FBRM) probe (Mettler Toledo® model E25) was placed vertically in the vessel, distant 10 mm downwards out from the stirrer shaft and equidistant from two baffles. The experimental set-up is shown in Figure 2.

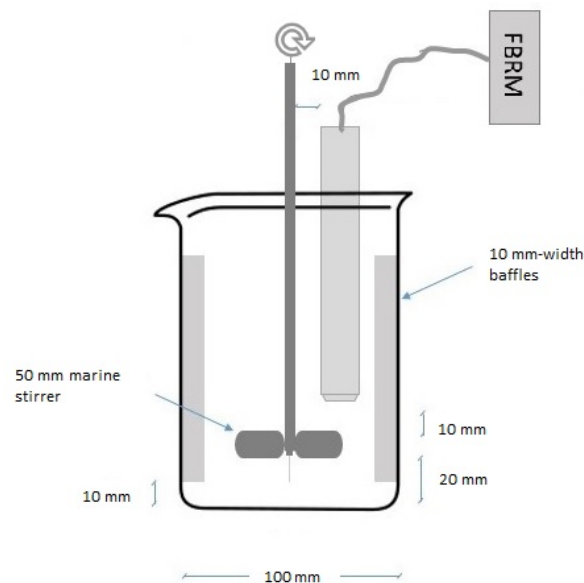


Figure 2. Schematic diagram of the stirred vessel used for the flocculation experiments.

The FBRM equipment works under the principle of laser back-scattering. A laser beam is focused to a small spot at a sapphire window, spinning at a tangential velocity of 2 m/s. When the laser beam hits a particle, the beam is reflected back to the probe window, inducing a peak of the signal until the particle leaves the path of the beam. The product of the peak duration and the tangential velocity of the spinning laser characterises the chord length and is recorded and counted in a corresponding size channel, thus generating the CLD. Complete reviews of the performance characteristics of this kind of equipment are given by Heath et al. [20] and Senaputra et al. [21] while, more recently, the application to continuous feed systems is discussed by Kyoda et al. [22].

The duration of mixing for the dispersion of solids and flocculation were 19.5 and 0.5 min, respectively, with a total experiment time of 20 min. The procedure was as follows—the dry powder (tailings or tailings/kaolin mixture) and the solution (water or salt-water) were mixed in the stirred vessel at a constant rate of 500 rpm for 19.5 min. Starting the last minute of the experiment (at 19.0 min), a known volume of diluted flocculant (prepared at 0.025 wt.%), enough for the required flocculant dosage of the experiment, was gently mixed in 0.1 dm^3 of solution separately (second dilution). 30 s before finishing the experiment (e.g., 19.5 min), the mixing rate was adjusted to the target value (60–500 rpm), depending on the test and then the diluted flocculant was put into the vessel, thus initiating the flocculation process.

The mean shear rate as a descriptor of mixing was characterised using the average velocity gradient (G) in turbulent regime and the circulation time (t_c related with the frequency of exposure of the aggregates to the impeller zone), as described by Spicer et al. [19] and Zhu et al. [23].

The parameter G is described by:

$$G = \left(\frac{\epsilon}{\nu} \right)^{1/2}, \quad (1)$$

where ν is the kinematic viscosity of the liquid and ϵ is the average turbulent energy dissipation rate:

$$\epsilon = \frac{N_p N^3 D^5}{V}. \quad (2)$$

Here, $N_p = 0.32$ is the power number of the impeller [24], N the impeller speed, D the diameter of the impeller and V the reaction volume.

The circulation time (t_c) is described by:

$$t_c = \frac{V}{N_q N D^3}, \quad (3)$$

where N_q denotes the dimensionless impeller pumping capacity (here, $N_q = 0.6$ [24]).

All measurements are well within a turbulent regime. Defining the impeller Reynolds number as:

$$Re = (ND^2)/\nu, \quad (4)$$

with ν the kinematic viscosity of water. With this definition, values between about 2600 and 14,000, corresponding to turbulent flow regime [25] have been found.

2.1.2. Settling Tests

Once the flocculation stage described in Section 2.1.1 was completed, the slurry was gently poured into a graduated cylinder (0.5 dm³, 50 mm diameter), with which settling rate measurements were made. Homogenisation was done by slowly inverting the cylinder twice, as described by McFarlane et al. [26].

The initial settling rate was measured by video analysis using a post-processing code written in GNU Octave, which identifies the position of the *mud line* (i.e., the supernatant-suspension interface) every 0.3 s. The flocculated suspension was let to settle for 300 s and then 0.02 dm³ of the supernatant sample was extracted for turbidity measurements (in nominal turbidity units, or NTU) by using a Hach[®] 18900 Turbidity Meter.

2.1.3. Zeta Potential

The Zeta potential (ZP) measurements of kaolin suspensions and the supernatant from settling tests were carried out at different solid concentrations using a Stabino[®] ParticleMetrix instrument.

The Stabino equipment has a measurement cell with a constant frequency oscillating piston. When a sample is put in the cell, the colloidal particles adsorb at the surface of the measuring cell by van der Waals forces and their counter ions stay in motion as a diffuse charge cloud around the attached particles. The movable counterions surrounding each particle follow the oscillation of the piston and induces an alternating voltage. The cloud potential (also called streaming potential) is detected and measured by two electrodes as a voltage measurement from which a streaming zeta potential (SZP) is obtained. According to the Helmholtz-Smoluchowski equation, the SZP is proportional to the ZP of the solid [27].

The supernatant from settling tests of pure tailings samples in distilled water was collected and then allowed to settle for two days. Then the solution was collected, and the solid content in the solution was dried for one day at 70 °C. Finally, the dry supernatant solid was diluted at different concentrations and was submitted to ZP measurements. For kaolin samples, several dilutions were made directly to the powder before ZP measurements.

2.2. Chemometric Analysis

To analyse the effects of solid concentration (C_p), flocculant dosage (FD) and mixing rate (MR) on the settling rate and supernatant turbidity, a response surface methodology (RSM) based on Doehlert experimental design was applied.

The RSM allows us to find optimum process conditions by exploring correlations between the different factors (i.e., C_p , FD and MR) and their responses (i.e., settling rate and supernatant turbidity). The RSM combine statistical and mathematical tools and it is based on the fit of a polynomial equation to the experimental data (a detailed description of the topic can be found in Lundstedt et al. [28] and references therein). The stages in this approach were—(1) selection of the experimental factors (i.e., C_p , FD and MR) and region of analysis, (2) choice of the experimental design and laboratory testing, (3) fitting of data to the polynomial function using mathematical-statistical analysis, (4) evaluation of model fitness, (5) verification of the region used in the analysis and (6) calculation of the optimum conditions (based on the objectives of the process) and definition of the optimum values for each factor [29]. The region of analysis that represents the range of each factor (e.g., for C_p the range of analysis was between 6% and 14%) was chosen based on a set of preliminary experiments.

The choice of a Doehlert experimental design (second stage in the RSM) as the chemometric approach was made because (a) it meets the requirements to apply a RSM , (b) it is a practical methodology and (c) it is an economical alternative for experimental studies of multiple variables at different number of levels [29]. This method has the advantage of capturing non-linear responses, which are commonly found in flocculation phenomena. According to this method, a second-order response function is defined to investigate both the main effects of the factors (or input variables) and their interaction, thus focusing only on those having the most substantial impact on the responses.

In a Doehlert design, the number of experiments is defined by $k^2 + k + 1$, where k represents the number of factors. In this case, the factors are C_p , FD and MR giving a set of 13 experiments. One of the properties of the Doehlert design is that 12 of the 13 experiments are uniformly distributed in a three-dimensional space sphere with a unit radius, all equidistant from a central point that represents the central experiment (number 13), based on average experimental conditions [30]. Figure 3 shows the geometrical solid formed, which is called cuboctahedron and the different tests generated by the location of its vertices.

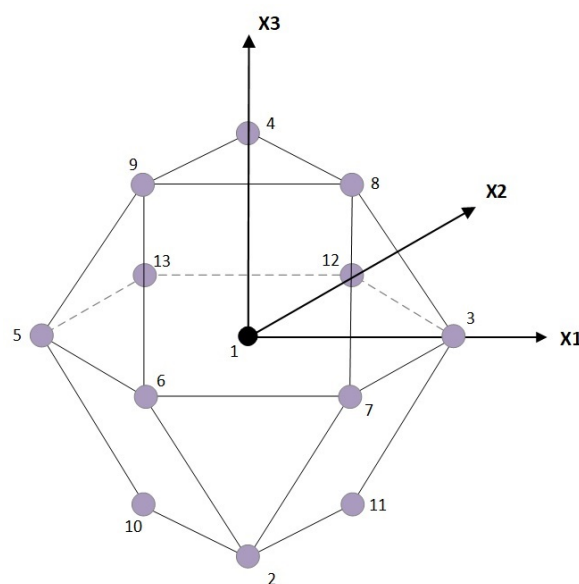


Figure 3. Doehlert designs for the optimization of three variables [29]. The cuboctahedron exhibits the location of the 13 experimental points in a three-dimensional space.

The number of levels of each factor was 5 for flocculant dosage (between 25 g/t and 35 g/t), 7 for mixing rate (between 70 rpm and 200 rpm) and 3 for solids concentration (between 6 wt.% and 14 wt.%). Table 2 shows the experimental matrix used in the current study, both as natural coded values (where 0 is the mean and -1 and 1 are the minimum and maximum values, respectively) and as real values used in those experiments including the corresponding average velocity gradient (G) for each MR value.

Table 2. Doehlert matrix response surface design for flocculant dosage (FD, x_1), mixing rate (MR, x_2) and solid concentration (C_p, x_3).

Exp	Coded Values			Experimental Values			
	x_1	x_2	x_3	FD	MR	G	C_p
	[-]	[-]	[-]	[g/t]	[rpm]	[1/s]	[%]
1	0	0	0	30.0	135	51.2	10.0
2	1	0	0	35.0	135	51.2	10.0
3	0.5	0.866	0	32.5	191	86.4	10.0
4	0.5	0.289	0.816	32.5	154	62.3	13.3
5	-1	0	0	25.0	135	51.2	10.0
6	-0.5	-0.866	0	27.5	79	22.8	10.0
7	-0.5	-0.289	-0.816	27.5	116	40.9	6.7
8	0.5	-0.866	0	32.5	79	22.8	10.0
9	0.5	-0.289	-0.816	32.5	116	40.9	6.7
10	0	0.577	-0.816	30.0	173	74.0	6.7
11	-0.5	0.866	0	27.5	191	86.4	10.0
12	-0.5	0.289	0.816	27.5	154	62.3	13.3
13	0	-0.577	0.816	30.0	97	31.4	13.3

The experimental values (E_i) were calculated from the coded values (x_i) by $E_i = E_{0i} + x_i \times \Delta E_i$, where E_{0i} is the centred value (or average) and ΔE_i the range. For FD , $E_{0i} = 30$ g/t and $\Delta E_i = 5$ g/t; for MR , $E_{0i} = 135$ rpm and $\Delta E_i = 65$ rpm; and for C_p , $E_{0i} = 10\%$ and $\Delta E_i = 4\%$.

To separate and estimate the sources of variation on each response (settling rate and turbidity, separately), an analysis of variance (ANOVA) was performed. In this analysis the observed variance in the response is partitioned into separate components related with each effect and interaction (i.e., C_p , FD , MR , C_p - C_p , C_p - FD , C_p - MR , FD - FD , FD - MR and MR - MR). Then each component is statistically tested to prove its significance.

Once the statistical analysis is made and significant effects detected, a regression equation is fitted to the data, where a model is obtained to describe each response based on the different effects and its interactions.

A (multiple response) optimisation analysis was made to search the global optimum on the response variables, where a desirability function methodology (DSM) was performed. This methodology allows an optimisation problem of two responses to be solved (in this case settling rate and turbidity of the supernatant) based on multiple factors or process conditions (here C_p , FD and MR).

The DSM is based on a desirability function that involves the transformation of each estimated response variable to a dimensionless value (d_i) in a scale between $d = 0$, for a completely undesirable response and $d = 1$ for a fully desired response [31]. There are different forms to obtain d_i depending on the target value (e.g., maximum, minimum or other value). By using dimensionless parameters, it is possible to combine the results obtained for properties measured on different orders of magnitude [29]. Once individual desirabilities are defined, an overall desirability (D) is calculated using each d_i in order to obtain its weighted geometric average ($D = \sqrt[m]{d_1 d_2 \dots d_m}$, where m is the number of responses).

Analysing the data response for settling rate and turbidity separately allows assessment of whether each of the estimated effects and interactions are statistically significant and if they have a positive or negative effect.

In the present work, the RSM analysis was performed by using the statistical software program *Statgraphics Centurion 18*, version 18.1.06 (Statpoint Technologies, Inc., Manugistics, Rockville, MD, USA).

3. Results and Discussion

3.1. Settling Rate

In the flocculation process, the first stage is the chemical interaction between the particles and the polymer (by adsorption) promoted by the mixing conditions. Then, adsorbed polymers tails that project into the solution and other particles give rise to the formation of aggregates [32].

Figure 4 (left panel) shows settling rates obtained at different average velocity gradients (G), for tailings and tailings/kaolin mixture (80/20 wt.%) in distilled water, 0.17 M NaCl solution (10 g/L, representing moderate salinity) and seawater. In most cases, a maximum in the mean setting rate was observed at $G \sim 50$ 1/s. This value of G is similar to that reported by Addai-Mensah et al. [14], who used a Couette cell and pure kaolinite with 250 g/t of a commercial anionic polyacrylamide.

Figure 4 (right panel) shows the circulation time (t_c). Results show that, up to $t_c \sim 0.05$ min, a relatively longer time of exposure of the aggregates to the impeller has a stronger positive impact on settling rate than shorter times.

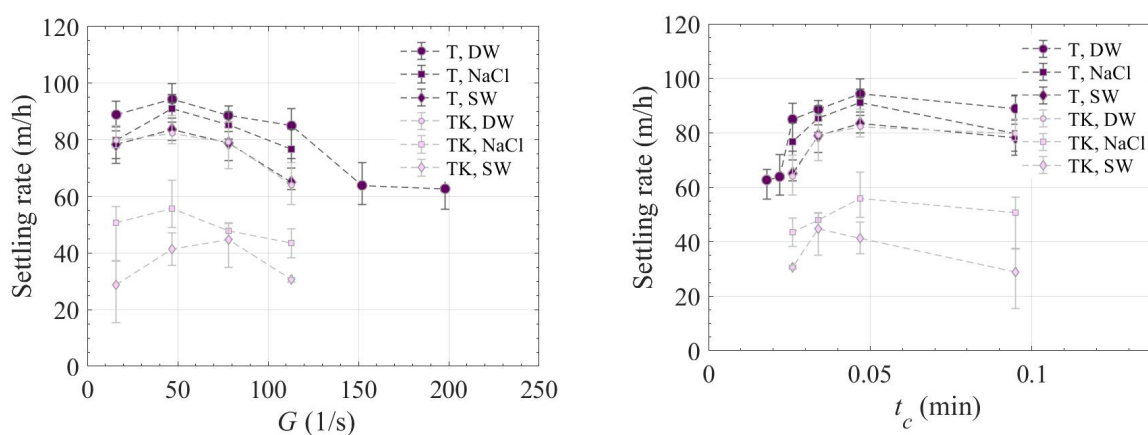


Figure 4. Settling rate (SR) versus average velocity gradient (G) (left) and circulation time (t_c) (right), for Tailings (T, dark colour markers) and Tailing/kaolin mixture (TK, light colour markers) in distilled water (DW, \circ), 0.17 M NaCl (\square) and seawater (SW, \diamond). The error bars represent minimum and maximum values. In all cases, $C_p = 7\%$ and the flocculant addition consisted of 30 g/t of PAM-A (SNF 704).

The prevailing mixing conditions promote the growth of aggregates and thus, more effective solid-liquid separation. However, if the mixing rate is too high, the turbulent shear forces can break the aggregates, and the separation efficiency might, therefore, decrease since smaller fragments will settle at lower rates. This is shown in Figure 4. One question here is the effect (or impact) on settling rate of a flocculant dosage increase (e.g., as a typical plant operational response when faced with overflow turbidity problems). This analysis was made using chemometrics tools and it is presented in Section 3.4.

Figure 4 also shows consistently lower values of the settling rate in the presence of salt. This is probably due to the shielding of the charge functionality of the flocculant preventing it from taking on an extended conformation (i.e., somewhat contracting its coil structure in solution) which limits its capacity to form larger aggregates by bridging [10,33], thereby reducing settling rates.

This behaviour was more marked when kaolinite and salt were added together, either as NaCl or seawater. This can be explained by the flocculant adsorption through the amide functionality by hydrogen bonding to the neutral surface groups, which in the case of kaolinite are located mainly at

the edges of its structure, where a higher proportion of aluminol groups (that provide the neutral sites) are present [34]. The edge area of the kaolinite is significantly lower compared to its faces [5,35] and other particles present in the pure tailings; also the kaolinite particles provide extra fine particles to the system, also negatively affecting the settling rate.

By combining both adverse effects—flocculant shielding functionality when salt is added and the diminishing of the available bonding surface when kaolinite is present—the results are lower settling rates, impacting the dewatering performance significantly.

3.2. Relationship between Chord Length and Settling Rate

The classical Stokes settling rate model, even when it is adapted to flocculated systems, suggests that the settling rate is roughly proportional to the square of the effective particle size [36]. This implies that there should be a monotonic relationship between the settling rate (i.e., the result of the settling test) and the chord length measurements using FBRM [21].

Figure 5 presents the data obtained in experiments at $G \sim 50$ 1/s, confirming the expected trend. However, it can be seen that similar chord length ranges may be related to significantly different settling velocities depending on the presence of kaolinite. This is explained by the different aggregate shapes when kaolinite is added, featuring a tendency to form flake structures [37], in contrast to the more spherical aggregates found in the pure tailings system which have a lower diameter and higher density, inducing higher settling rates.

This change in the structure shape might be explained by the electrostatic repulsion between flocculant and kaolinite faces and also due to the low flocculant adsorption mechanism (as was described above), thus generating voluminous aggregates with a more porous structure, as mentioned by Nabzar et al. [38].

The presence of salt diminished the aggregate size. This is explained by the reduced bridging capacity of the flocculant promoted by the polymer shielding in the presence of salt.

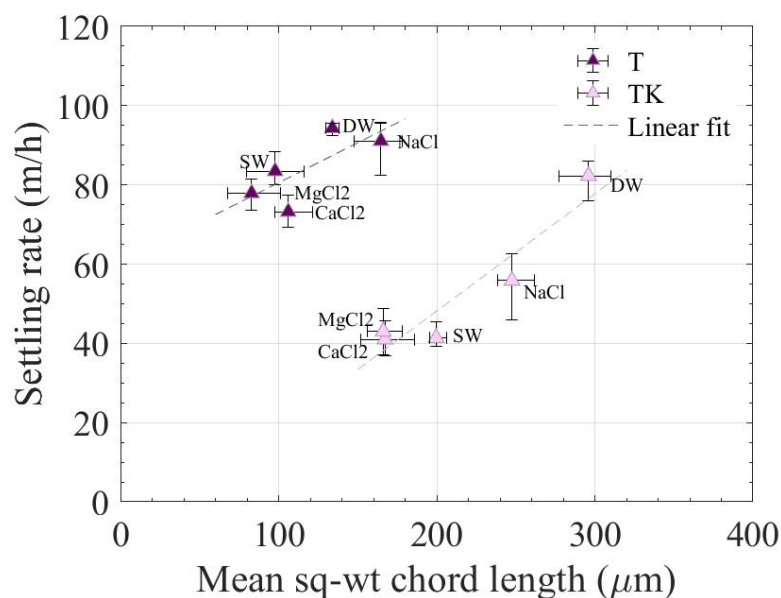


Figure 5. Settling rate (SR) vs. average squared weighted chord length (L_c) for tailings (T, dark colour \triangle) and tailings/kaolin mixture (TK, light colour \triangle) in distilled water (DW), NaCl 10 g/L, seawater (SW), CaCl₂ 1.1 g/L and MgCl₂ 4.8 g/L. In all cases, $C_p = 7\%$, the flocculant addition consisted of 30 g/t of PAM-A (SNF 704) and $G \sim 50$ 1/s.

3.3. Turbidity of the Supernatant

When comparing the experiments made with pure tailings in distilled water with those containing 20% kaolin, it was found that the turbidity of the supernatant achieved in the latter is much lower, after a period of 300 s of sedimentation.

Figure 6 (left panel) shows that the mixing rate and the presence of kaolin and salts change the turbidity (and thus the presence of suspended solids) in the supernatant. The observed reduction in supernatant turbidity as the mixing rate was increased is explained by the combination of residence time in the reactor and an increased probability of bridging collision between particles with adsorbed flocculant due to velocity fluctuations inside the reactor promoted by mixing, as predicted by classical orthokinetic theory [32].

In the absence of kaolinite, ZP measurements made on the supernatant after settling tests correspond to $ZP \sim -40$ mV, while the ZP of the kaolin sample was close to -20 mV. These results suggest electrostatic repulsion between negatively charged tailings particle surface (that are probably high in quartz content) and the dosed polymer hinder adsorption of the latter and thus contribute to higher supernatant turbidity once the settling process is finished. This situation changes when kaolinite is present, as at the pH of the experiments (~ 4.9) the clay phase is likely to present a heterogeneous charge, leading to a heterocoagulation process with the remainder of the minerals that make up the tailings, driven by an electrostatic attraction of its neutral sites.

Experiments in the saline medium generated lower supernatant turbidity compared to those in distilled water, because the presence of salts causes a coagulant effect of the primary particles before to their interaction with the polyelectrolytes is induced and, consequently, a small proportion of fine particles is present in the supernatant suspension. The experiments carried out with seawater resulted in lower supernatant turbidity compared to the experiments in NaCl, due to the high salinity of the seawater compared with the NaCl solution used (seawater 0.6 M vs. NaCl 0.17 M). Also, divalent cations such as Ca^{2+} and Mg^{2+} (present in the seawater) are more efficient in the screening of the anionic charge of the particles [39], thereby increasing the probability of forming aggregates by coagulation. The result is a reduction of turbidity according to the sequence distilled water > NaCl solution > seawater.

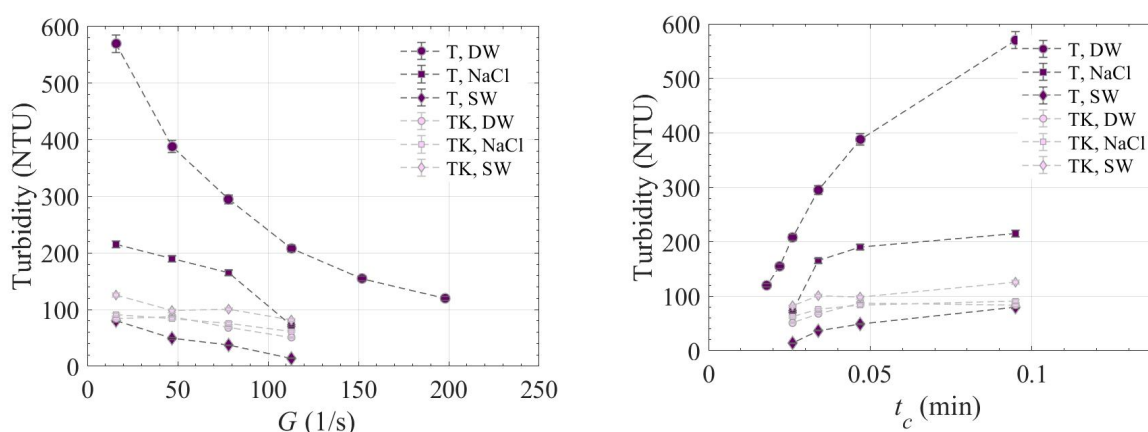


Figure 6. Turbidity versus average velocity gradient G (left) and circulation time (right), for tailings (T, dark colour markers) and tailings/kaolin mixture (TK, light colour markers) in distilled water (DW, \circ), NaCl 10 g/L (\square), seawater (SW, \diamond). In all cases, $C_p = 7\%$ and the flocculant addition consisted of 30 g/t of PAM-A (SNF 704).

3.4. Chemometric Analysis for Optimum Flocculation Response

Under the experimental conditions indicated above in Table 2, orthokinetic flocculation optimisation provides improvements on the settling rate and turbidity of the supernatant, but the mixing conditions that maximise settling rates are different than those required to minimise the

turbidity of the supernatant. In most mineral processing plants, the only equipment used to control tailings flocculation is the thickener, with the only dynamic adjustment available often being the flocculant dosage. This is a practice that can often be highly inefficient, leading to excessive flocculant consumption and negative impacts on underflow properties. Alternatively, thickening could be complemented with an additional turbidity removal process, for which there are several low footprint equipment options [40].

The lack of correspondence between input conditions for concurrently higher settling rates and higher solids overflow (or turbidity) removal was more marked in the case of tailings without kaolinite, as revealed using the *RSM* approach. Figure 7 shows a Pareto chart with the result of such analysis with 90% confidence level.

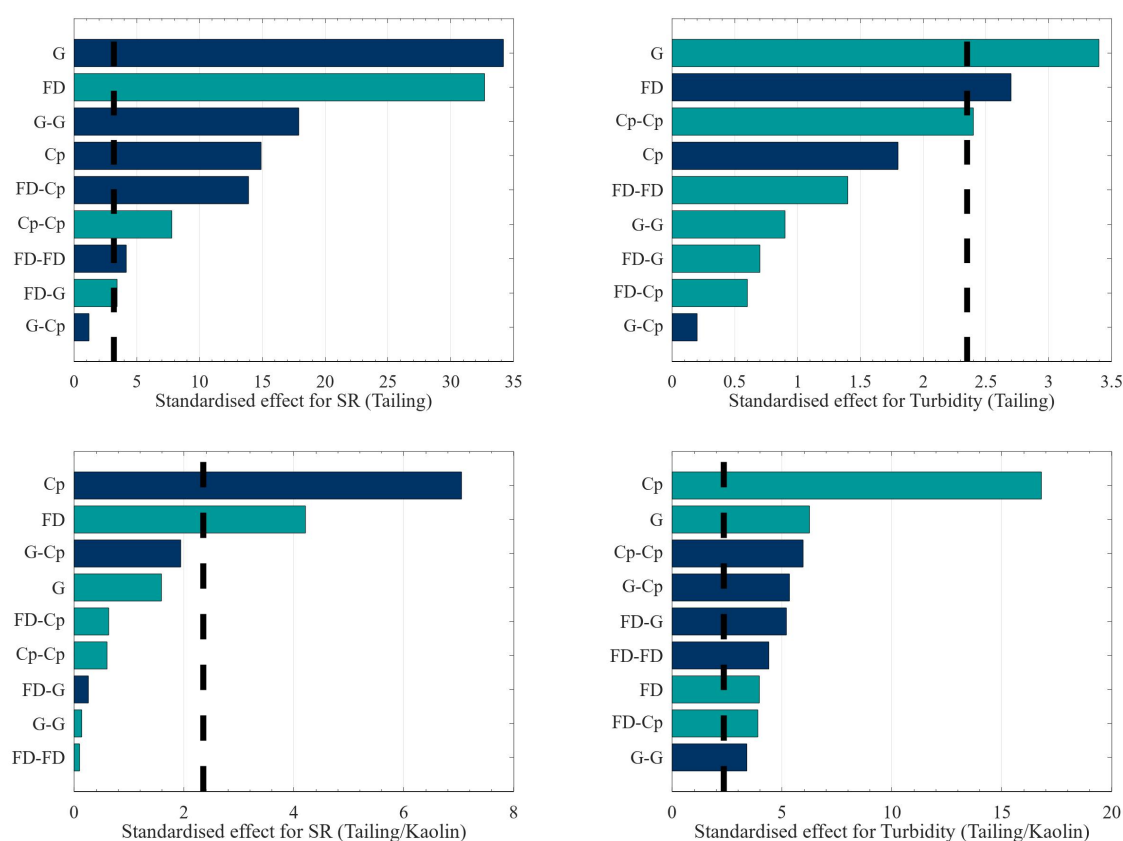


Figure 7. Standardised (normalised) Pareto chart for settling rate (*SR*) and turbidity of the supernatant, showing the main effect of flocculant dosage (*FD*), average velocity gradient (*G*) and solid concentration (C_p) (light and dark bar colours denote positive and negative effect, respectively). The significance level (α) corresponds to the vertical dashed line, while bars extending to right of it denote statistically significant data.

Figure 7 shows that, among all the analysed effects, the average velocity gradient *G* has the main (although opposite) impact on settling rate and supernatant turbidity responses, in pure tailings experiments. Also, the flocculant dosage (*FD*) gives an important contribution to the flocculation performance. For the tailings/kaolin mixture experiments, the main effect was due to the solid concentration, C_p , while the secondary effect for settling rate was flocculant dosage and for turbidity was *G*. The Pareto chart confirms that the mixing rate is a relevant variable in the measured flocculation responses but only for pure tailings experiments. It also indicates that C_p is a relevant variable when a significant fraction of kaolinite (or presumably any other clay) is present in the ore.

Contours of the estimated surface response for pure tailings experiments and tailings/kaolin mixtures was obtained in order to investigate the different effects on each response.

Figure 8a shows the contours of the estimated surface response for tailings experiments carried out in distilled water at $C_p = 10\%$, while Figure 8b shows the corresponding surface response for tailings/kaolin mixtures with $G = 50$ 1/s (the most significant variables were chosen for each case). The results reveal that the mixing rate and the flocculant dosage conditions that generate the optimum value (denoted by crosses in the figure) for settling rate (maximum) are quite different from those for turbidity removal (crosses denoting minima). In the case of the tailings/kaolin mixture, the behaviour was qualitatively similar, showing that the optimum dilution conditions for settling rate are different than those for turbidity removal.

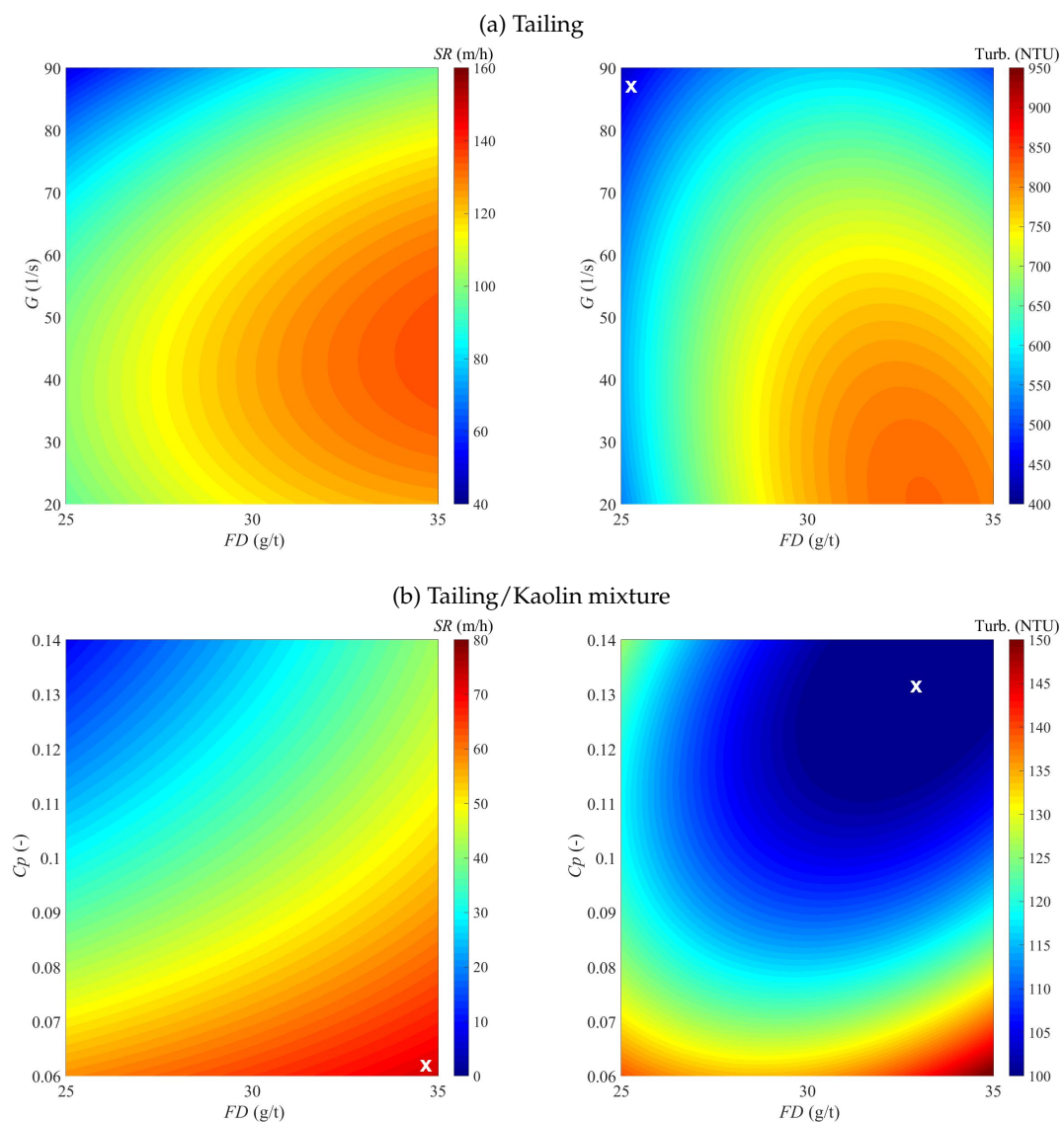


Figure 8. Contours of the estimated response surface (CRS) corresponding to the most sensitive variable conditioning settling velocity (left) and turbidity (right) for (a) tailings (shown FD and G in the x - and y -axis, respectively) and (b) tailings/kaolin mixture (shown FD and C_p in the x - and y -axis, respectively). In (a), the CRS represents conditions for $C_p = 10\%$, while in (b), the mixture the conditions are for $G = 50$ 1/s. Crosses denote the optimum values.

In both examples ($C_p = 10\%$ for tailings in distilled water and $G = 50$ 1/s for tailing/kaolin mixtures in distilled water), the multiple response optimisation analysis gives an extended area for the best desirability number which is also low, ~ 0.4 and ~ 0.7 for each type of material. This means that both the tailings thickening and the turbidity removal processes will be sub-optimal

when both responses are required to be near their optimum values within the same unit process (thickening-clarification), being a necessary compromise between the required flocculation conditions at the feedwell and the mineral characteristics.

The global multiple response optimisation procedure used in this work reveals that the maximum desirability value is 0.98 and 0.86 for tailings and tailings/kaolin mixtures, respectively. Table 3 summarise the results obtained with the RSM analysis, showing that the same FD is required to achieve the maximum SR and minimum turbidity, although with different values of G and C_p . It can be noted, however, that the minimum and maximum values of turbidity removal in tailings/kaolin are similar and both low. Therefore, by removing the minimum turbidity restriction, the maximum settling rate is obtained at the same optimum G as in pure tailings experiments.

Table 3. Multiple response optimisation results for Tailing and Tailing/kaolin mixture.

Descriptor	Tailing	Tailing/Kaolinite
Min SR , m/h	72	15.6
Max SR , m/h	153	64.7 (*)
Min Turbidity, NTU	491	100
Max Turbidity, NTU	810	135
Optimum values:		
SR , m/h	150	51.5
Turbidity, NTU	491	94.1
Desirability	0.98	0.86
FD , g/t	35	35
G , 1/s	70	23
C_p , %	6.8	12.6

(*) Corresponds to conditions of experiment #10.

When comparing the experiments made with pure tailings in distilled water with those containing 20% kaolin (Table 3 and Figure 8), it was found that the turbidity of the supernatant achieved in the latter is much lower. While with the pure tailings optimal turbidity of 491 NTU was achieved, the tailings with kaolin reached 94 NTU.

The settling rate of the experiments with pure tailings was higher than in the case when clay is present (see Table 3 and Figure 8); while with a pure tailings the optimum settling rate was 150 m/h, for the tailings with clays the settling rate was 52 m/h (notice that these values of settling rates are higher than the necessities in a typical thickening operation). The reverse trend could be expected considering that the system with clay has a previous heterocoagulation that facilitates the action of the flocculant; however, the irregular morphology of the kaolinite assigns a greater surface area than the rest of the particles that make up the tailings (mainly quartz), and therefore it demands a higher consumption of flocculant, without contributing mostly to the formation of new flocculant-particles bridges. On the other hand, the aggregate size is more significant when kaolinite was present. This indicates that the aggregates generated in the presence of kaolinite have a lower density, which would be responsible for the low sedimentation rate. Unlike turbidity, the Pareto chart indicates that, in terms of settling rate efficiency, the flocculant has a substantial importance in both particle systems.

4. Conclusions

In most copper sulphide mining operations, where water recovery needs to be optimised, maximising particle settling rate is often an operational priority. However, in some cases, low solid content or turbidity in the overflow is also an operational target due to the negative impact of the fine fraction both in the water transport system and in the flotation plant [41].

Chemometric analyses represent an economical method that helps to reduce time and materials when seeking to find optimum values of input parameters and also to understand the complexity of treating minerals of differing behaviour. Through chemometric analysis, it was possible to determine the optimal conditions of the process, in terms of two responses relevant for thickening—settling rate

and turbidity of the supernatant. Although in practice, it is necessary to find the operational conditions that optimise both responses, this cannot always be achieved at the same time because the mechanisms that govern both variables are different.

By analysing the Pareto chart, it could be demonstrated that the mixing rate and the flocculant dosage are the most critical variables for turbidity in the case of pure tailings; meanwhile, the behaviour of the tailings mixed with kaolin was controlled mainly by the solid concentration and the mixing rate (with a minor effect of the flocculant dosage), suggesting that heterocoagulation phenomenon was more important in defining turbidity than the extent of aggregation.

It could also be shown that mixing conditions have a strong influence on the settling rate. When the intensity of mixing increases, there is a higher probability of bridging collisions between particles. However, increasing the mixing rate promotes the breakage of the aggregates and consequently reduces their size. These competitive phenomena lead to the identification of an optimal settling rate, independent of the mineralogy of the tailings or type of water and confirm previous experimental findings.

While a saline medium promotes a positive effect on the quality of the overflow (e.g., reduce turbidity), it promotes a negative effect on the settling rate. Independent of the mineralogy, distilled water promotes faster settling in both cases (with and without kaolinite). The lowest values were obtained with seawater and CaCl_2 and MgCl_2 .

It is proposed that the presence of divalent cations leads to a more significant detriment on the capacity of the flocculant [42]. The divalent cations interact with the anionic functional groups of polyacrylamide, reducing its ability to generate flocculant-particle bridges and, therefore, the size of the aggregates.

The present study highlights the necessity to establish a compromise between the settling rate and the capture of fines if the feedwell is used as the sole flocculation process in thickening. Those opposing outcomes of the thickening operation could be optimised by splitting them, with a thickener as a first process and then followed by a secondary fine solids removal stage from the overflow. A techno-economical study would clarify the extent of the implications of reducing flocculant consumption at the thickening stage.

Author Contributions: Conceptualization, C.C. and C.F.I.; methodology, C.C.; validation C.C., R.I.J. and C.F.I.; investigation, C.C. and C.F.I.; resources, C.F.I.; writing, original draft preparation, C.C., C.F.I. and R.I.J.; writing, review and editing, R.I.J.; visualization, C.C.; supervision, C.C. and C.F.I.; project administration, C.F.I.; funding acquisition, C.F.I.

Funding: CSIRO-Chile International Centre of Excellence in Mining (Innova CSIRO-Chile 10ECII-9007), CONICYT Fondecyt Project No. 1160971 and CONICYT/PIA Project AFB180004.

Acknowledgments: The authors thank financial support from CSIRO-Chile International Centre of Excellence in Mining (Innova CSIRO-Chile 10ECII-9007) and the Chilean National Commission for Science and Technology, CONICYT, through Fondecyt Project No. 1160971 and CONICYT/PIA Project AFB180004. The authors also thank the Laboratory for Rheology and Fluid Dynamics of the Department of Mining Engineering Universidad de Chile for technical support and Prof. Mercedes Becerra-Herrera for her valuable insights on the chemometric analysis.

Conflicts of Interest: The authors declare no conflict of interest.

References

1. Ihle, C.F.; Tamburrino, A. Variables affecting energy efficiency in turbulent ore concentrate pipeline transport. *Miner. Eng.* **2012**, *39*, 62–70. [[CrossRef](#)]
2. Ihle, C.F.; Kracht, W. The relevance of water recirculation in large scale mineral processing plants with a remote water supply. *J. Clean. Prod.* **2018**, *177*, 34–51. [[CrossRef](#)]
3. Herrera-León, S.; Lucay, F.A.; Cisternas, L.A.; Kraslawski, A. Applying a multi-objective optimization approach in designing water supply systems for mining industries. The case of Chile. *J. Clean. Prod.* **2019**, *210*, 994–1004. [[CrossRef](#)]
4. Boger, D.V. Rheology and the resource industries. *Chem. Eng. Sci.* **2009**, *64*, 4525–4536. [[CrossRef](#)]

5. Nasser, M.; James, A. The effect of polyacrylamide charge density and molecular weight on the flocculation and sedimentation behaviour of kaolinite suspensions. *Sep. Purif. Technol.* **2006**, *52*, 241–252. [[CrossRef](#)]
6. Zbik, M.S.; Smart, R.S.C.; Morris, G.E. Kaolinite flocculation structure. *J. Colloid Interface Sci.* **2008**, *328*, 73–80. [[CrossRef](#)] [[PubMed](#)]
7. Ndlovu, B.; Forbes, E.; Farrokhpay, S.; Becker, M.; Bradshaw, D.; Deglon, D. A preliminary rheological classification of phyllosilicate group minerals. *Miner. Eng.* **2014**, *55*, 190–200. [[CrossRef](#)]
8. Ji, Y.; Lu, Q.; Liu, Q.; Zeng, H. Effect of solution salinity on settling of mineral tailings by polymer flocculants. *Colloids Surf. A Physicochem. Eng. Asp.* **2013**, *430*, 29–38. [[CrossRef](#)]
9. Jeldres, R.; Toledo, P.; Concha, F.; Stickland, A.; Usher, S.; Scales, P. Impact of seawater salts on the viscoelastic behavior of flocculated mineral suspensions. *Colloids Surf. A Physicochem. Eng. Asp.* **2014**, *461*, 295–302. [[CrossRef](#)]
10. Jeldres, R.I.; Leiva, W.H.; Toledo, P.G.; Piceros, E.C.; Herrera, N. Viscoelasticity and yielding properties of flocculated kaolinite sediments in saline water. *Colloids Surf. A Physicochem. Eng. Asp.* **2017**, *529*, 1009–1015. [[CrossRef](#)]
11. Svarovsky, L. Chapter 14—Solid–liquid separation–thickening. In *Mineral Processing Design and Operations*, 2nd ed.; Gupta, A., Yan, D., Eds.; Elsevier: Amsterdam, The Netherlands, 2000; pp. 471–506.
12. Šulc, R.; Dittl, P. Scale-up rules for flocculation. *Int. J. Miner. Process.* **2017**, *167*, 79–85. [[CrossRef](#)]
13. Mpofo, P.; Addai-Mensah, J.; Ralston, J. Flocculation and dewatering behaviour of smectite dispersions: Effect of polymer structure type. *Miner. Eng.* **2004**, *17*, 411–423. [[CrossRef](#)]
14. Addai-Mensah, J.; Yeap, K.; McFarlane, A. The influential role of pulp chemistry, flocculant structure type and shear rate on dewaterability of kaolinite and smectite clay dispersions under couette Taylor flow conditions. *Powder Technol.* **2007**, *179*, 79–83. [[CrossRef](#)]
15. Botha, L.; Soares, J. The influence of tailings composition on flocculation. *Can. J. Chem. Eng.* **2015**, *93*, 1514–1523. [[CrossRef](#)]
16. Bulatovic, S.; Wyslouzil, D.; Kant, C. Effect of clay slimes on copper, molybdeum flotation from porphyry ores. In Proceedings of the Copper 99-Cobre 99 International Environment Conference—Volume II, Phoenix, AZ, USA, 10–13 October 1999; pp. 96–111.
17. Wang, C.; Harbottle, D.; Liu, Q.; Xu, Z. Current state of fine mineral tailings treatment: A critical review on theory and practice. *Miner. Eng.* **2014**, *58*, 113–131. [[CrossRef](#)]
18. Massart, D.; Vandeginste, B.; Deming, S.; Michotte, Y.; Kaufman, L. *Chemometrics: A Textbook*, 5th ed.; Data Handling in Science and Technology—Volume 2; Elsevier Science: Budapest, Hungary, 2003.
19. Spicer, P.T.; Keller, W.; Pratsinis, S.E. The effect of impeller type on floc size and structure during shear-induced flocculation. *J. Colloid Interface Sci.* **1996**, *184*, 112–122. [[CrossRef](#)] [[PubMed](#)]
20. Heath, A.; Fawell, P.; Bahri, P.; Swift, J. Estimating average particle size by focused beam reflectance measurement (FBRM). *Part. Part. Syst. Charact.* **2002**, *19*, 84–95. [[CrossRef](#)]
21. Senaputra, A.; Jones, F.; Fawell, P.; Smith, P. Focused beam reflectance measurement for monitoring the extent and efficiency of flocculation in mineral systems. *AIChE J.* **2014**, *60*, 251–265. [[CrossRef](#)]
22. Kyoda, Y.; Costine, A.D.; Fawell, P.D.; Bellwood, J.; Das, G.K. Using focused beam reflectance measurement (FBRM) to monitor aggregate structures formed in flocculated clay suspensions. *Miner. Eng.* **2019**, *138*, 148–160. [[CrossRef](#)]
23. Zhu, Z.; Wang, H.; Yu, J.; Dou, J. On the kaolinite floc size at the steady state of flocculation in a turbulent flow. *PLoS ONE* **2016**, *11*, e0148895. [[CrossRef](#)]
24. Furukawa, H.; Kato, Y.; Inoue, Y.; Kato, T.; Tada, Y.; Hashimoto, S. Correlation of power consumption for several kinds of mixing impellers. *Int. J. Chem. Eng.* **2012**, *2012*, 106496. [[CrossRef](#)]
25. Paul, E.; Atiemo-Obeng, V.; Kresta, S. *Handbook of Industrial Mixing: Science and Practice*, 3rd ed.; John Wiley and Sons, Inc.: Hoboken, NJ, USA, 2004.
26. McFarlane, A.; Bremmell, K.; Addai-Mensah, J. Optimising the dewatering behaviour of clay tailings through interfacial chemistry, orthokinetic flocculation and controlled shear. *Powder Technol.* **2005**, *160*, 27–34. [[CrossRef](#)]
27. Elimelech, M.; Chen, W.; Waypa, J. Measuring the zeta (electrokinetic) potential of reverse osmosis membranes by a streaming potential analyzer. *Desalination* **1994**, *95*, 269–286. [[CrossRef](#)]
28. Lundstedt, T.; Seifert, E.; Abramo, L.; Thelin, B.; Nystrom, A.; Pettersen, J.; Bergman, R. Experimental design and optimization. *Chemom. Intell. Lab. Syst.* **1998**, *42*, 3–40. [[CrossRef](#)]

29. Bezerra, M.A.; Santelli, R.E.; Oliveira, E.P.; Villar, L.S.; Escalera, L.A. Response surface methodology (RSM) as a tool for optimization in analytical chemistry. *Talanta* **2008**, *76*, 965–977. [[CrossRef](#)] [[PubMed](#)]
30. Doehlert, D. Uniform Shell Designs. *J. R. Stat. Soc. Ser. C (Appl. Stat.)* **1970**, *19*, 231–239. [[CrossRef](#)]
31. Derringer, G.; Suich, R. Simultaneous optimization of several response variables. *J. Qual. Technol.* **1980**, *12*, 214–219. [[CrossRef](#)]
32. Gregory, J. Polymer adsorption and flocculation in sheared suspensions. *Colloids Surf.* **1988**, *31*, 231–253. [[CrossRef](#)]
33. Quezada, G.; Jeldres, R.; Fawell, P.; Toledo, P. Use of molecular dynamics to study the conformation of an anionic polyelectrolyte in saline medium and its adsorption on a quartz surface. *Miner. Eng.* **2018**, *129*, 102–105. [[CrossRef](#)]
34. Lee, L.; Rahbari, R.; Lecourtier, J.; Chauveteau, G. Adsorption of polyacrylamides on the different faces of kaolinites. *J. Colloid Interface Sci.* **1991**, *147*, 351–357. [[CrossRef](#)]
35. Taylor, M.; Morris, G.; Self, P.; Smart, R. Kinetics of adsorption of high molecular weight anionic polyacrylamide onto kaolinite: The flocculation process. *J. Colloid Interface Sci.* **2002**, *250*, 28–36. [[CrossRef](#)] [[PubMed](#)]
36. Richardson, J.; Zaki, W. Sedimentation and fluidisation: Part I. *Chem. Eng. Res. Des.* **1997**, *75*, S82–S100. [[CrossRef](#)]
37. Du, J.; Morris, G.; Pushkarova, R.; Smart, R. Effect of surface structure of kaolinite on aggregation, settling rate, and bed density. *Langmuir* **2010**, *26*, 13227–13235. [[CrossRef](#)] [[PubMed](#)]
38. Nabzar, L.; Pefferkorn, E.; Varoqui, R. Polyacrylamide-sodium kaolinite interactions: Flocculation behavior of polymer clay suspensions. *J. Colloid Interface Sci.* **1984**, *102*, 380–388. [[CrossRef](#)]
39. Israelachvili, J.N. *Intermolecular and Surface Forces*, 3rd ed.; Academic Press: New York, NY, USA, 2011.
40. Reyes, C.; Ihle, C.; Apaz, F.; Cisternas, L. Heat-assisted batch settling of mineral suspensions in inclined containers. *Minerals* **2019**, *9*, 228. [[CrossRef](#)]
41. Wang, Y.; Peng, Y.; Nicholson, T.; Lauten, R. The different effects of bentonite and kaolin on copper flotation. *Appl. Clay Sci.* **2015**, *114*, 48–52. [[CrossRef](#)]
42. Witham, M.; Grabsch, A.; Owen, A.; Fawell, P. The effect of cations on the activity of anionic polyacrylamide flocculant solutions. *Int. J. Miner. Process.* **2012**, *114–117*, 51–62. [[CrossRef](#)]



© 2019 by the authors. Licensee MDPI, Basel, Switzerland. This article is an open access article distributed under the terms and conditions of the Creative Commons Attribution (CC BY) license (<http://creativecommons.org/licenses/by/4.0/>).